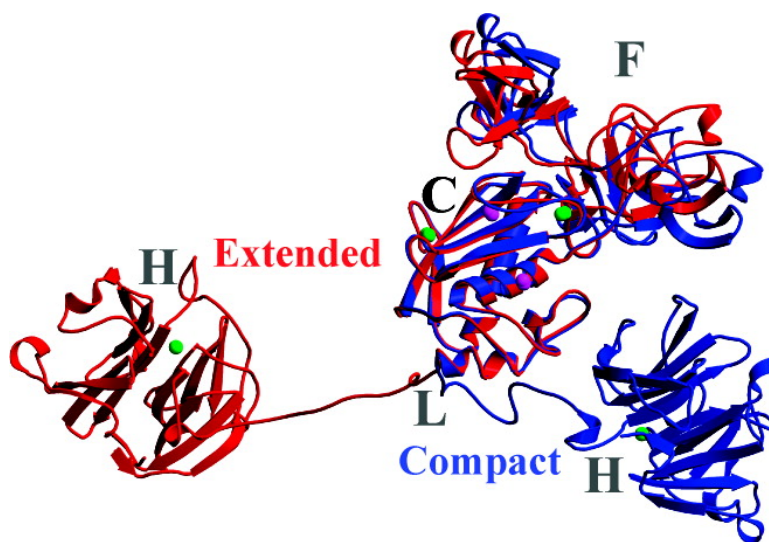Communication

From the X-ray Compact Structure to the Elongated Form of the Full-Length MMP-2 Enzyme in Solution: A Molecular Dynamics Study

Natalia Di#az, Dimas Sua#rez, and Haydee Valde#s

More About This Article

Additional resources and features associated with this article are available within the HTML version:

- Supporting Information
- Access to high resolution figures
- Links to articles and content related to this article
- Copyright permission to reproduce figures and/or text from this article

View the Full Text HTML

From the X-ray Compact Structure to the Elongated Form of the Full-Length MMP-2 Enzyme in Solution: A Molecular Dynamics Study

Natalia Díaz,* Dimas Suárez, and Haydee Valdés

Universidad de Oviedo, Dpto. Química Física y Analítica, C/ Julián Clavería, 8, 33006 (Oviedo) Asturias, Spain

Received August 3, 2008; E-mail: diazfnatalia@uniovi.es

Matrix metalloproteinases (MMPs) are an important family of zinc- and calcium-dependent peptidases involved in the regulation of the cellular behavior by proteolytic processing of the pericellular environment.[1] These metalloenzymes are multidomain proteins composed, in most cases, by a catalytic and a hemopexin-like domains joint together by a linker of variable length.[2] X-ray structures of the full-length enzymes are currently available for MMP-1 and MMP-2.[3] These solid-state structures display the different domains in a similar compact arrangement, which clearly suggests the presence of stable interdomain contacts. However, small-angle X-ray scattering and atomic force microscopy experiments have shown that significant interdomain motions occur for the MMP-9 in solution.[4] Very recently, nuclear magnetic resonance measurements performed for MMP-12 have also shown that the catalytic and hemopexin-like domains experience conformational freedom with respect to each other on the ns time scale.[5] Thus, it seems that the MMPs can adopt a manifold of conformations in solution.

To obtain further structural insight into the conformations accessible to a full-length MMP in aqueous solution, we study in this work the MMP-2 enzyme, which is a key player in angiogenesis that has been validated as an anticancer drug target.[6] In addition to the catalytic (**C**) and hemopexin-like (**H**) domains, the MMP-2 enzyme possesses three fibronectin-type domains (**F1**−**F3**) inserted in the sequence of the catalytic domain, and a linker region (**L**) connecting the **C** and **H** domains which comprises ∼20 amino acids. Initial coordinates for the active enzyme were obtained from the 1CK7 full-length pro-MMP-2 crystal structure (2.8 Å resolution).[3] The total system (551 residues plus two Zn(II) and three Ca(II) ions) was embedded in a large octahedral box containing more than 37 000 water molecules to allow ample interdomain motions. The molecular dynamics (MD) simulation was extended up to 100 ns. Further details relative to the setup of the system and the simulation protocol are provided in the Supporting Information.

We observed that, all along the MD simulation, the internal structure of the **C** and **H** domains remained quite stable according to the computed root mean squared deviations (rmsd's) of the backbone heavy atoms with respect to the X-ray structure: 1.03 ± 0.07 and 1.51 ± 0.12 Å, respectively. The corresponding rmsd values for the three fibronectin-type domains are 1.36 ± 0.17, 1.67 ± 0.18, and 2.62 ± 0.41 Å. The absence of the propeptide segment in the active enzyme, which interacts with **F3** in the crystal structure, explains the larger value obtained for this domain. However, the global rmsd computed for the whole protein backbone exhibits a sharp increase (from 4 to 30 Å) within the 70−75 ns time frame. Similarly, the radius of gyration plotted as a function of time evolves smoothly at ∼28 Å during the first three-quarters of the trajectory and then it increases up to 45 Å, signaling thus a dramatic change in the interdomain arrangement of the MMP-2 system.

Before discussing the reorientation of the MMP-2 domains, we will briefly comment on the nature and relative stability of the interdomain interactions. During the first 70 ns of simulation time, the relative orientation of the MMP-2 domains remains quite close to that observed in the X-ray structure thanks to a combination of polar and hydrophobic interactions. On one hand, residues Leu$_{508}$ and Ala$_{510}$ from the first propeller blade of the **H** domain give hydrophobic contacts (see Table S1) with the side chains of Thr$_{426}$ and Thr$_{428}$ from the Ω-loop of the **C** domain. These interactions result in a moderate reduction (243 ± 43 Å^2) of the solvent-excluded molecular surface of the two domains. A larger patch of molecular surface (360 ± 94 Å^2) is covered by the packing of 12 linker residues against the Ω-loop of the **C** domain, resulting in several interdomain H-bonds (e.g., Gln$_{435}$-NH···Pro$_{463}$-O, Asp$_{416}$-Oδ···Thr$_{465}$-OγH) and hydrophobic interactions (Pro$_{417}$···Thr$_{465}$). The smallest interdomain contact region is formed between the second blade of the **H** domain and **F1**. The only **F1**−**H** interaction is a solvent-exposed salt-bridge (Glu$_{243}$···Arg$_{550}$), which alternates between direct (59%) and water-mediated (33%) H-bonds. On the other hand, the root mean squared flexibility of the **L** region in the compact conformation is quite high (2.4 ± 0.5 Å), which is in consonance with the lack of electron density for Asp$_{450}$-Thr$_{460}$ in the 1CK7 structure. Nevertheless, secondary structure analyses assign a helical conformation to the first residues, Asp$_{450}$-Leu$_{453}$, and distinguish in ∼50% of the analyzed snapshots two bend regions with a high curvature at the Gly$_{454}$-Thr$_{458}$ and Thr$_{460}$-Leu$_{461}$ segments, followed by an irregular loop, Gly$_{462}$-Glu$_{467}$, adjacent to the **H**-domain.

According to our MD calculations, the first interdomain interaction that is irreversibly lost through thermal fluctuations of solvent and protein atoms is the Glu$_{243}$···Arg$_{550}$ salt bridge, which is located in the **F1**−**H** contact region. Once this contact is lost at 70 ns, the **C**−**H** interface becomes more solvent-exposed, destabilizing thus the hydrophobic interactions between the two domains. As the **C**−**H** contact surface diminishes, the flexible **L** region experiences two conformational changes: (a) between 74−76 ns the Thr$_{460}$-Leu$_{461}$ segment adopts an extended conformation through backbone torsional motions (see Figures S1 and S2); (b) the conformation of Gly$_{456}$ changes at 77 ns resulting in an extended coil from Gly$_{454}$ to Glu$_{467}$.

The loss of the interdomain interactions, as well as the conformational changes of the **L** region, results in a remarkable rearrangement of the **H** domain with respect to **C** and **F1**−**F3** (see Figure 1a). As shown in Figure 1b, the separation between the **C** and **H** centers of mass doubles from 70 to 90 ns, going from 39 to 80 Å. We also computed the Euler angles that characterize the relative orientation of two rigid coordinate systems placed at the center of mass of the **C** and **H** domains, respectively (see Figure 1c). The polar plots of the ϕ, θ, and ψ angles clearly show that the separation of the **C** and **H** domains is accompanied by an important rotational motion of the **H** domain with respect **C**. During the final 10 ns of the simulation, the MMP-2 enzyme maintains a fully
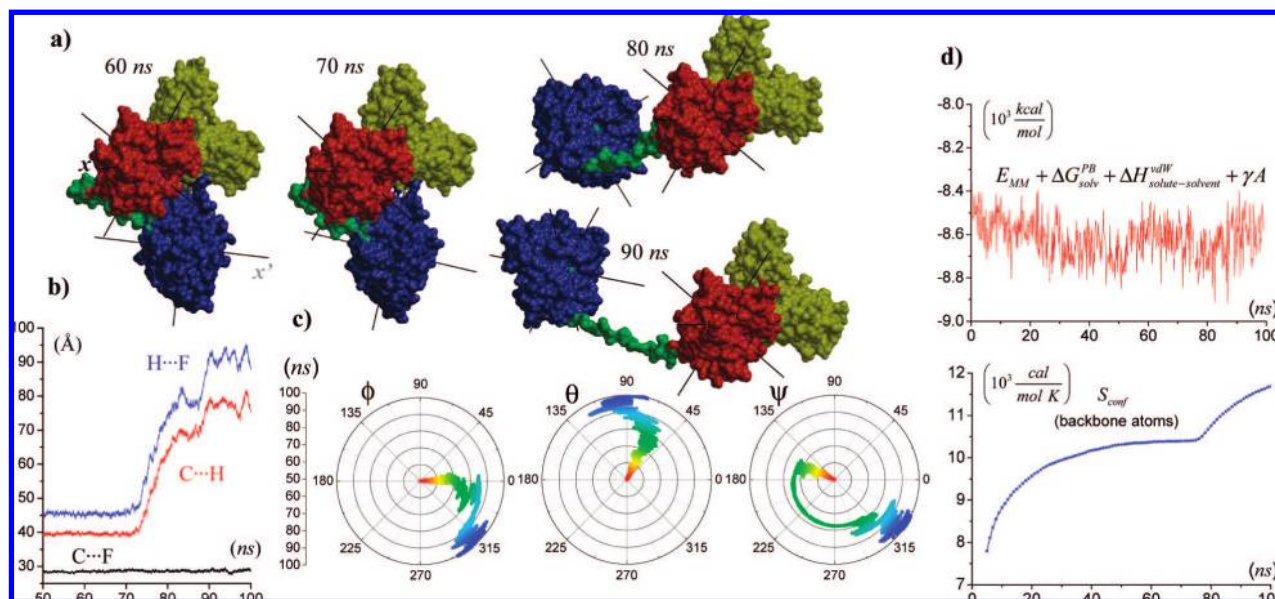
Figure 1. (a) Molecular surface representation of the catalytic (in red), fibronectins (in yellow), linker (in green), and hemopexin (in blue) domains at different simulation times. The axes of the coordinate systems centered at the catalytic and hemopexin domains are also displayed. (b) Interdomain distances (Å) between the center of mass of the catalytic (**C**), fibronectin (**F**), and hemopexin (**H**) domains. (c) Dial plots of the Euler rotational angles (in degrees; *xyx* convention) of the **H** domain with respect to **C**. The *x*-axis of **C** is parallel to the axis running along the α2 helix, while the *x'*-axis of **H** runs along the central channel of the β-propeller structure. (d) Solute energy plus solvation free energy and configurational entropy plots.

elongated form, which differs significantly from that observed in the solid-state structure.

We also estimated the evolution of the energy of the solvated MMP-2 enzyme by combining the molecular mechanics (MM) potential energy of the protein with its electrostatic Poisson–Boltzmann (PB) solvation energy and the nonpolar contributions computed from its surface area and the vdW interactions with explicit solvent (see Figure 1d). The MM-PB energy tended to decrease during the first 30 ns and then remains stable up to 70 ns, fluctuating at ~ −8658 (4) kcal/mol (standard error in parentheses). When the **C** and **H** domains are well separated during the final 20 ns, the average MM-PB energy increases, −8620 (11) kcal/mol, suggesting thus that the loss of interdomain interactions is not compensated by a larger solvent stabilization. To investigate the role played by entropy, we computed the configurational entropy (S_{conf}) of the backbone atoms all along the MD trajectory by means of the Schlitter approximation. As seen in Figure 1d, the S_{conf} plot converges slowly toward a limiting value of ~10 400 cal/mol K corresponding to the MMP-2 in its compact form. However, an important jump in S_{conf} occurs when the enzyme starts elongating, which is most likely due to the larger fluctuations of the interdomain structural parameters (Figure 1b–c).

Unfortunately, we cannot predict a reliable free energy difference between the compact and the elongated forms of the MMP-2 in solution due to the approximations involved in the entropic calculations and the limited sampling. Nevertheless, our results suggest that the thermodynamic force driving the MMP-2 system in solution from the X-ray compact structure to the elongated form would be entropic. In this way, it can be reasonably expected that the solvated MMP-2 enzyme would have access to a statistical ensemble of conformations spanned by the fluctuations of the interdomain structural parameters.

In summary, as previously found experimentally for MMP-9 and MMP-12,[4,5] our simulation shows that extended configurations are accessible for the full-length MMP-2 enzyme in solution. Our structural and energetic analyses give fresh insight into how and why the interdomain interactions change during the transition from the compact to the elongated form and add support to the hypothesis that the reorientation of the **C** and **H** domains in solution is a common feature of the MMPs. Eventually, the computational models of the extended MMP-2 enzyme could also be useful for modeling protein assemblies involved in the regulation and/or the collagenolytic activity of the MMPs.[7]

Supporting Information Available: Computational Methods. Table S1. Figures S1–S2. A 60 Mb MPEG-2 movie showing the 70–90 ns time interval. Representative MD snapshots in PDB format. This material is available free of charge via the Internet at http://pubs.acs.org.

References

(1) Sternlicht, M. D.; Werb, Z. *Ann. Rev. Cell. Dev. Biol.* **2001**, *17*, 463–516.
(2) Maskos, K. *Biochimie* **2005**, *87*, 249–263.
(3) Morgunova, E.; Tuuttila, A.; Bergmann, U.; Isupov, M.; Lindqvist, Y.; Schneider, G.; Tryggvason, K. *Science* **1999**, *284*, 1667–1670.
(4) Rosenblum, G.; et al. *Structure* **2007**, *15*, 1227–1236.
(5) Bertini, I.; Calderone, V.; Fragai, M.; Jaiswal, R.; Luchinar, C.; Melikian, M.; Mylonas, E.; Svergun, D. *J. Am. Chem. Soc.* **2008**, *130*, 7011–7021.
(6) Overall, C. M.; Kleifeld, O. *Nat. Rev. Cancer* **2006**, *6*, 227–239.
(7) Perumal, S.; Antipova, O.; Orgel, J. P. R. O. *Proc. Natl. Acad. Sci. U.S.A.* **2008**, *105*, 2824–2829.

JA806090V